NASA TECHNICAL NOTE

NASA TN D-4801

NASA TN D-4801

A SEMIGRAPHICAL METHOD FOR A DEORBIT TRAJECTORY DESIGN STUDY

by Richard N. Green, William F. Hampshire II, and Sue W. Souders

Langley Research Center
Langley Station, Hampton, Va.

NATIONAL AERONAUTICS AND SPACE ADMINISTRATION • WASHINGTON, D. C. • OCTOBER 1968

A SEMIGRAPHICAL METHOD FOR A DEORBIT TRAJECTORY DESIGN STUDY

By Richard N. Green, William F. Hampshire II,
and Sue W. Souders

Langley Research Center
Langley Station, Hampton, Va.

NATIONAL AERONAUTICS AND SPACE ADMINISTRATION

For sale by the Clearinghouse for Federal Scientific and Technical Information
Springfield, Virginia 22151 – CFSTI price $3.00

A SEMIGRAPHICAL METHOD FOR A DEORBIT TRAJECTORY DESIGN STUDY

By Richard N. Green, William F. Hampshire II,
and Sue W. Souders
Langley Research Center

SUMMARY

A semigraphical method to aid in the selection of a deorbit trajectory which is compatible with arbitrarily selected mission constraints is presented. The method is applicable to the case where the initial orbit about the planet and the deorbit trajectory are coplanar. Basically, the method consists of examining a family of candidate trajectories and eliminating, by a graphical cross-plotting technique, those which violate the mission constraints. In addition, the trade-offs which exist between the various demands on the trajectory become graphically obvious. The method is flexible in that the user is free to dictate the mission mode and the mission constraints. An example illustrating the use of the method for a Mars mission is presented.

INTRODUCTION

Man has long sought to understand and explore the solar system around him. In recent years, considerable knowledge of the neighboring planets has been obtained from interplanetary probes. These missions have consisted of instrumented space vehicles which passed close to the planets while proceeding in orbits about the Sun. Therefore, experiments to obtain planetary information were short in duration. A likely candidate for future exploration involves placing satellites in orbits about the planets whereupon experiments can be performed over long periods of time. Surface probes can be ejected from such a satellite orbit to gather more comprehensive planetary data. This procedure requires a velocity maneuver to transfer the probe to a descent trajectory. Therefore the combined use of the orbiting satellite and the ejected surface probe seems a likely candidate for use in interplanetary exploration in the near future. The descending probe may be required to satisfy a number of constraints imposed by the mission goals, the subsystem requirements, or by the laws of physics. In the final result, these considerations must be integrated into a workable and mutually compatible spacecraft system. Eventually, the spacecraft orbit and the probe trajectory must be designed to satisfy the mission objectives within the constraints imposed by the entire set of subsystems. There is a requirement, therefore, to determine a method of examining the many facets of such a complex mission.

The intent of this report is to present a semigraphical method to aid in the selection of descent trajectories which are compatible with the mission constraints. To reduce the complexity of the general three-dimensional problem, the motion of the probe has been assumed to remain in the plane of the satellite orbit. This assumption would seem to be reasonable since considerably more fuel would have to be expended to establish an out-of-plane trajectory. Basically, the method consists of examining a family of reasonable trajectories and eliminating, by a graphical cross-plotting technique, those which violate the mission constraints. In addition, the trade-offs which exist between the various demands on the trajectory become graphically obvious. A discussion of the method and its use for various mission modes is given. Finally, the method is applied to a hypothetical Mars mission and results in the identification of a family of descent trajectories which satisfy all the imposed constraints over a range bounded by two Martian atmospheric models.

SYMBOLS

A	cross-sectional area, meters^2
C_D	drag coefficient
f	true anomaly of deorbit, degrees (see fig. 1(a))
h	altitude of probe, meters (see fig. 1(c))
h_a	apoapsis altitude of satellite orbit, kilometers (see fig. 1(a))
h_d	altitude of probe at parachute deployment, meters
h_p	periapsis altitude of satellite orbit, kilometers (see fig. 1(a))
l	television footprint length, meters (see fig. 1(c))
m	mass, kilograms
m/C_DA	ballistic coefficient of probe before parachute deployment, kilograms/meter^2
$(m/C_DA)_d$	ballistic coefficient of probe-parachute system after parachute deployment, kilograms/meter^2
V	velocity of probe, meters/second (see fig. 1(b))

ΔV	magnitude of deorbit velocity maneuver, meters/second (see fig. 1(a))
β_l	angle at probe measured from local vertical to line of sight to satellite, degrees (see fig. 1(b))
γ	flight-path angle of probe, degrees (see fig.1(b))
γ_e	γ of probe at limiting altitude of atmosphere, degrees
$\Delta\nu_{l,max}$	maximum change in ν_l during parachute descent phase, degrees
θ	application angle of ΔV measured from satellite negative velocity vector at deorbit, degrees (see fig. 1(a))
ν_l	angle at probe measured from probe's negative velocity vector to line of sight to satellite, degrees (see fig. 1(b))
$\nu_{l,d}$	ν_l at parachute deployment, degrees
$\nu_{l,min}$	minimum ν_l during parachute descent phase, degrees
Φ	position angle of probe at impact referenced to periapsis of satellite orbit and considering no atmosphere during descent, degrees
Φ_t	position angle of probe at impact referenced to periapsis of satellite orbit and considering an atmosphere during descent, degrees (see fig. 1(a))
ψ	any relative position angle between probe and satellite
ψ_1	lower constraint on ψ
ψ_2	upper constraint on ψ

SEMIGRAPHICAL METHOD

For the purpose of illustrating the method, consider the following mission mode and and mission constraints. The mission mode consists of a velocity maneuver out of orbit, aerodynamic deceleration, and parachute braking near the terminal phase. The parachute is to be deployed at a specific Mach number. To insure a survivable impact on the

surface of the planet, the altitude at which deployment occurs is restricted to be above some minimum altitude h_d. Assume that the communication system requires that a relative position angle ψ between the probe and the satellite be bounded at impact for the purposes of transmitting surface data to the satellite. Therefore, the position angle at impact is constrained between ψ_1 and ψ_2. These constraints could cover a number of different situations and are defined here in general terms for the purpose of illustration. The size and shape of the orbit have been defined along with the position in orbit at which the deorbit maneuver is to be performed. In addition, the aerodynamics of the probe and the parachute system have been defined. The problem reduces to bounding the magnitude and direction of the velocity maneuver to produce a family of impacting trajectories which will permit the successful accomplishment of the mission and will simultaneously satisfy, or not violate, any of the imposed mission constraints.

Since the probe remains in the plane of the satellite orbit, the descent trajectory can be uniquely defined by two independent parameters once the initial orbit and the deorbit point have been fixed. These two independent parameters are of the utmost importance in the graphical representation of the deorbit geometry. The easiest ones to visualize are ΔV, the magnitude of the deorbit velocity maneuver, and θ, the angle of application (fig. 1(a)), since these are the control variables during the actual mission. Nevertheless, several different sets of parameters were examined, and by trial and error another set was found to be more useful for design purposes, namely, θ and the vacuum landing point on the surface. Consider sketch (a) where Φ is the vacuum landing point on

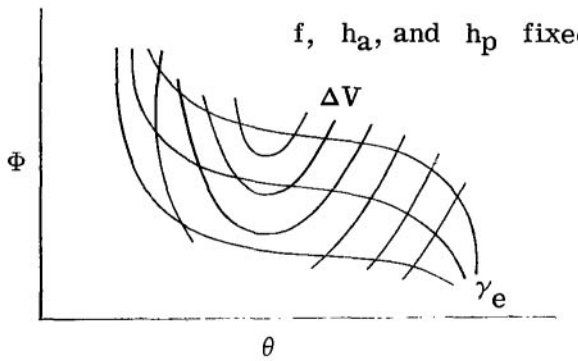

Sketch (a)

the surface measured from some reference line, taken here as the line of apsides of the initial orbit, and γ_e is the flight-path angle at atmospheric entry. Lines of constant ΔV and γ_e have been plotted as a function of Φ and θ. Notice that f, the true anomaly at deorbit; h_a, the apoapsis altitude; and h_p, the periapsis altitude have been fixed. Since the trajectory can be defined by Φ and θ, the sketch is a graphical representation of all possible descent trajectories. It remains to eliminate those areas which violate the mission constraints. These areas were eliminated by selecting a number of sample

trajectories that encompassed all possibilities. These sample trajectories corresponded to the intersections of the lines of constant ΔV and γ_e. For each sample trajectory the true landing point Φ_t was computed by numerically integrating the equations of motion through the atmosphere. The resulting landing point is displayed in sketch (b)

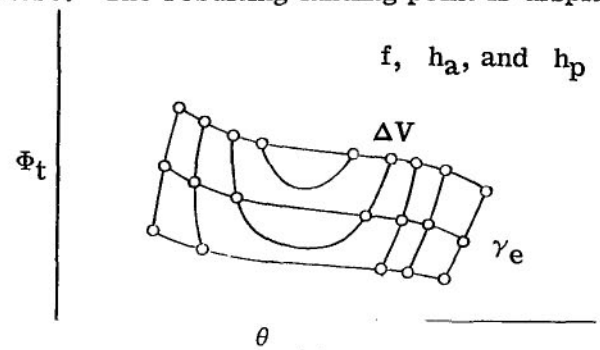

Sketch (b)

where the symbols represent the data points. Several of the sample trajectories have the same flight-path angle at atmospheric entry whereas other groupings have common values of ΔV at deorbit. This result is due to choosing the samples at the intersections of the constant γ_e and ΔV lines in sketch (a). By connecting the appropriate data points, lines of constant ΔV and γ_e were formed on the new coordinate plane. Thus, the $\Delta V, \gamma_e$ grid was plotted as a function of θ and an integrated parameter Φ_t. The approach of plotting the $\Delta V, \gamma_e$ grid against different parameters is the basis of the method presented here. In this manner the true landing point of all possible trajectories was found by examining only a few well chosen samples.

Consider the mission constraints to eliminate the undesirable trajectories. For example, the parachute system is restricted to deployment above h_d to insure a survivable impact. The computed altitude of parachute deployment for each sample trajectory was then plotted as a function of θ and the $\Delta V, \gamma_e$ grid was constructed (sketch (c)).

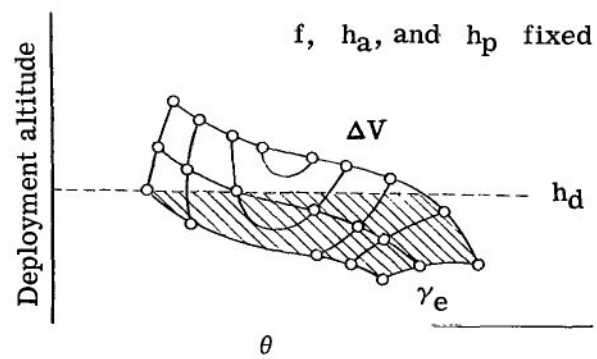

Sketch (c)

The trajectories within the shaded area violate the parachute deployment constraint and were eliminated from consideration. In a similar manner the position angle at impact was plotted as a function of Φ_t (sketch (d)). Only those trajectories which have a ψ at impact between ψ_1 and ψ_2 are acceptable from a communication point of view.

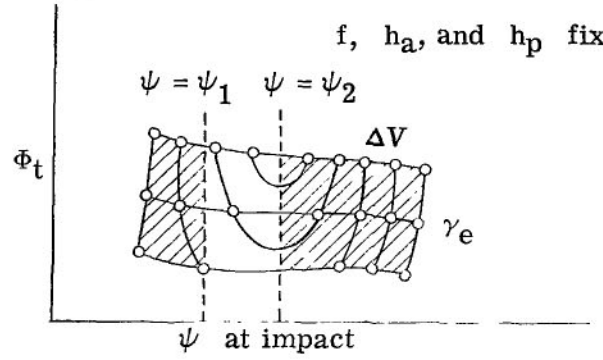

Sketch (d)

All constraint lines were then transferred to sketch (e) by means of the $\Delta V, \gamma_e$ grid which was common to all plots. In this way a family of descent trajectories was

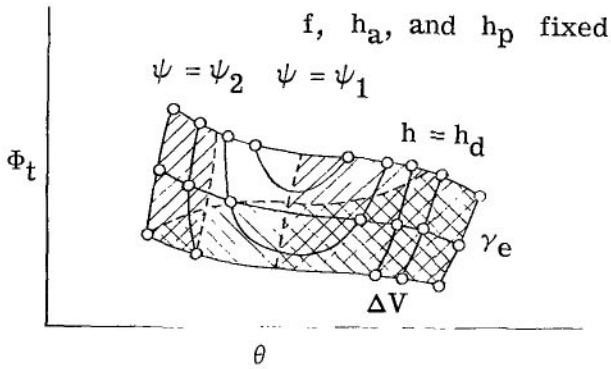

Sketch (e)

found which satisfied the mission objectives. Within this area, additional optimization can be made; that is, the most desirable descent trajectory can be selected. If the mission is overconstrained and all trajectories are eliminated, one must reexamine the various constraints to find a solution. This examination is immediately possible with the separate parametric plots (sketches (c) and (d)) without generating additional trajectory data.

To reiterate, a family of desirable descent trajectories was found for a given mission mode. The vacuum landing point and the deorbit velocity application angle were taken as the independent parameters to define the trajectory. A group of sample trajectories were chosen to represent various combinations of ΔV and γ_e and were then numerically integrated through the atmosphere. The undesirable trajectories were eliminated by examining the separate parametric plots associated with each constraint. The

constraint lines were then transferred to a common plot by means of the $\Delta V, \gamma_e$ grid. By this semigraphical method a family of descent trajectories which satisfied the mission constraints was found.

DISCUSSION OF METHOD

Normally, the mission mode and constraints are more complex than those in the illustrative example. Although only two constraints were considered, any number of constraints could have been imposed. Provided a parameter is single-valued along each trajectory, one can plot the parameter as a function of some appropriate secondary parameter and the $\Delta V, \gamma_e$ grid constructed. The secondary parameter should be chosen on the basis of the shape of the resulting $\Delta V, \gamma_e$ grid. It has been found that this choice has a great effect on the graphical representation of the data. The mission mode could have been extended to include a more sophisticated deployment criteria for the parachute. The use of thrusting rockets to slow the probe could have been included in the study. In any event, the procedure should prove to be applicable for more complex missions.

Many different parameters can be investigated by repetition of the method. The true anomaly which was held constant in the previous example is a case in point. The influence of the deorbit position on the selection of a descent trajectory could be investigated by repeating the same procedure with a different true anomaly. The family of satisfactory descent trajectories which result from the second iteration could be overlaid with those from the first. The result of this type of procedure would possibly lead to a smaller family of trajectories which satisfies the mission constraints over a region of deorbit true anomalies instead of only at one point. A similar study could be performed to investigate the influence of the size and shape of the satellite orbit. If the planet's atmosphere is not well defined, one may use the method to select a descent trajectory which insures the mission objectives over a range of atmospheric models.

Obviously, the method is very flexible in that the user is free to define the mission mode and the various constraints imposed on the descent trajectory. In addition, the method can be repeated to investigate the influence of various parameters. The difficulty in applying the method arises in the formulation of a given constraint so that it can be handled graphically as outlined. Many times this formulation will require some insight into the problem and some additional computations. More complex mission constraints are examined in the section devoted to the selection of a Mars descent trajectory. Because of the flexibility of the method, it should provide a logical, orderly procedure for a wide variety of studies.

NUMERICAL EXAMPLE

To illustrate the method further, a study to design the descent trajectory for a hypothetical Mars-probe mission is presented. The satellite and the probe are injected into an elliptical orbit about Mars from which the probe will separate from the satellite and at an appropriate time transfer to a descent trajectory by means of a small coplanar velocity maneuver. The probe is slowed down by using both atmospheric braking and a parachute to provide for a survivable impact. While the probe is descending on the parachute, a television system gathers imagery data of the surface and transmits it back to the satellite. Constraints pertaining to both the communication and the television subsystems are considered. In addition, the descent trajectory is chosen to insure a successful mission over a range of possible atmospheric models. The following numerical values are postulated for use throughout the numerical study.

(a) Periapsis altitude of the orbit, h_p, 1000 km

(b) Apoapsis altitude of the orbit, h_a, 20 000 km

(c) True anomaly of deorbit, f, 240^o

(d) Voyager Mars atmospheric models, VM-8 and VM-4

(e) Limiting altitude of the atmosphere, 243 840 m (800 000 ft)

(f) Ballistic coefficient of the probe before parachute deployment, m/C_DA, 39 kg/m^2 (0.25 $slug/ft^2$)

(g) Ballistic coefficient of the probe-parachute system after parachute deployment, $(m/C_DA)_d$, 3.8 kg/m^2 (0.024 $slug/ft^2$)

(h) Parachute is deployed at a Mach number of 1.6

(i) Parachute is released at an altitude of 1524 m (5000 ft)

(j) Television lens full field of view, 32^o

(k) Television coverage of the planet begins when ℓ = 9144 m (30 000 ft) (see fig. 1(c))

(l) Antenna on probe has a beam width of 60^o

The following mission constraints are imposed on the descent trajectory:

(a) $-20^o \leqq \gamma_e \leqq -15^o$

(b) $\Delta V \leqq 400$ m/s

(c) $0^o \leqq \theta \leqq 180^o$

(d) Altitude at which television coverage is initiated $\geqq$ 6096 m (20 000 ft)

(e) $-30^{o} \leqq \nu_{l} \leqq 30^{o}$ during parachute descent phase

(f) β_{l} at impact $\geqq -60^{o}$

(g) β_{l} at impact plus 5 minutes $\leqq 60^{o}$

The flight-path angle at atmospheric entry is bounded to avoid possible "skip-out" or excessive heating. The weight allocation has restricted the amount of fuel for the deorbit maneuver. The application angle of the velocity maneuver θ is applied so that the descent trajectory lies inside of the spacecraft orbit. If the velocity increment were applied in an outward direction, the probe would pass outside of the satellite orbit and then would cross the orbit before landing on the surface. This condition is avoided to eliminate possible communication problems. To avoid oblique imagery, the television coverage is initiated at an adequate altitude. In order to transmit these pictures to the satellite with a directional antenna, the descent trajectory is chosen so that the satellite will be in the proper position relative to the lander during the parachute descent. A measure of the satellite's position relative to the probe's body axis is the ν_{l} angle (fig.1(b)). Since the probe's antenna beam width is 60^{o}, the ν_{l} angle during the parachute descent is bounded between $\pm 30^{o}$. Low data rate communication is insured during the entire descent phase and for 5 minutes after impact. To insure that the communication is not broken because of the horizon or possible mountain ranges, the β_{l} angle (fig. 1(b)) at impact is greater than -60^{o}. Similarly, the β_{l} angle at 5 minutes after impact is not to exceed 60^{o}. These mission objectives and mission constraints are considered in the selection of a descent trajectory which will provide a successful mission within the range of Martian atmospheres assumed to be bounded by the VM-4 and VM-8 atmospheres.

The vacuum plot (fig. 2) was constructed to select the sample trajectories. At this point the constraints on γ_{e} and θ were considered, that is, sample trajectories were chosen so that γ_{e} was between -15^{o} and -20^{o} while θ was bounded between 0^{o} and 180^{o}. In addition, each sample had a ΔV of 400 m/s or less. Therefore, a group of sample trajectories was chosen which encompassed all reasonable candidates. Notice that the vacuum plot is independent of the atmospheric model and the mission mode because of the geometric and conic relationships between the four parameters, Φ, θ, γ_{e}, and ΔV. For this reason, the sample trajectories were applicable for the consideration of both the VM-8 and VM-4 atmospheres. The thinner VM-8 atmosphere was considered first. The sample trajectories were numerically integrated through the Martian atmospheres to obtain the parameters associated with each mission constraint. The true landing point which is dependent on both the atmospheric model and the mission constants such as the ballistic coefficients is presented in figure 3(a). The altitude constraint for the initiation of the television system was investigated with figure 3(b). Those trajectories which violated the two β_{l} angle constraints became obvious with the construction of figures 3(c) and 3(d). The constraint on the relative positions of the probe and satellite for

communication purposes was satisfied by consideration of figure 3(e). This plot will be discussed subsequently. The mission constraints as listed previously were satisfied by transferring all the constraint lines to a common plot and by eliminating those areas of the trajectories which violated any of the constraints. Therefore, the shaded area in figure 3(f) represents the family of descent trajectories that satisfied all the mission requirements in a VM-8 atmosphere.

The ν_l angle constraint restricted the descent trajectory to be chosen so that the ν_l angle was maintained between $\pm 30^o$ during the parachute descent phase. This constraint was not handled as the others were because the parameter of interest was bounded during a period of time and not at one specific point. Thus, a different approach was taken. Examination of the ν_l angle showed that the angle started decreasing immediately after parachute deployment and continued decreasing until a minimum was reached at which time it started increasing slowly until the end of the parachute phase was reached. The maximum value always occurred at deployment whereas the minimum value occurred at some other time during the parachute deceleration phase. Several different graphical representations were tried before figure 3(e) was considered. The abscissa is the value of ν_l at parachute deployment and the ordinate is the maximum variation of ν_l during the parachute phase. The vertical line at $\nu_{l,d} = 30^o$ is obviously one extreme of the usable area of trajectories. The other can be reasoned as follows. If the ν_l angle at deployment is 20^o, then the total change in ν_l must be less than 50^o ($\Delta\nu_{l,max} \geqq -50^o$) to insure that the minimum ν_l is greater than -30^o. This approach establishes the constraint line labeled "$\nu_{l,min} = -30^o$." These two lines bounded the area of descent trajectories which satisfied the constraint that $-30^o \leqq \nu_l \leqq 30^o$ during the parachute phase. From a communication viewpoint, the preferable condition would be equal angular excursions. This condition exists along the line labeled "$\nu_{l,balanced}$." Notice that this constraint was examined on a plot that contained neither Φ_t nor θ as the others did. Nevertheless, the constraint line was transferred to a common plot by use of the $\Delta V, \gamma_e$ grid.

The family of descent trajectories that satisfied all the mission requirements in the VM-4 atmosphere is represented by the shaded area in figure 4. The procedure followed was the same as previously outlined with the exception of the use of a different atmospheric model. The two areas from figures 3(f) and 4 were then transferred to the vacuum plot (fig. 5) since it was independent of the atmosphere. The common area, therefore, represents the descent trajectories that satisfy the mission constraints and provide for a successful mission over a range of possible Martian atmospheres bounded by VM-4 and VM-8 atmospheres.

One of the major advantages of the semigraphical method is the presentation of the various trade-offs that exist. Within the common area of descent trajectories, a choice of a specific trajectory can be made. If one desires a steep flight-path angle, the magnitude

of the deorbit velocity is increased and the probe is forced to land farther from the periapsis of the satellite orbit. If very shallow entry angles γ_e are desired the β_l constraint at impact plus 5 minutes could be relaxed. This trade-off between flight-path angle and communication time after impact and other similar trade-offs are byproducts of the constraint plots. These comparisons can be seen with no additional computation or plotting. It is very easy to overconstrain the descent trajectory; in which case, these trade-offs become increasingly important.

CONCLUDING REMARKS

A semigraphical method to aid in the selection of a descent trajectory has been presented. The method is flexible in that the user dictates both the mission mode and the mission constraints. A wide variety of studies can be performed by repeating the method for different mission parameters such as the dimensions of the satellite orbit, the position within the orbit of the deorbit maneuver, or the atmospheric model. The method expedites the selection of a descent trajectory since an orderly procedure has been established and a descriptive set of design plots have been found.

Langley Research Center,
National Aeronautics and Space Administration,
Langley Station, Hampton, Va., June 19, 1968,
789-30-01-01-23.

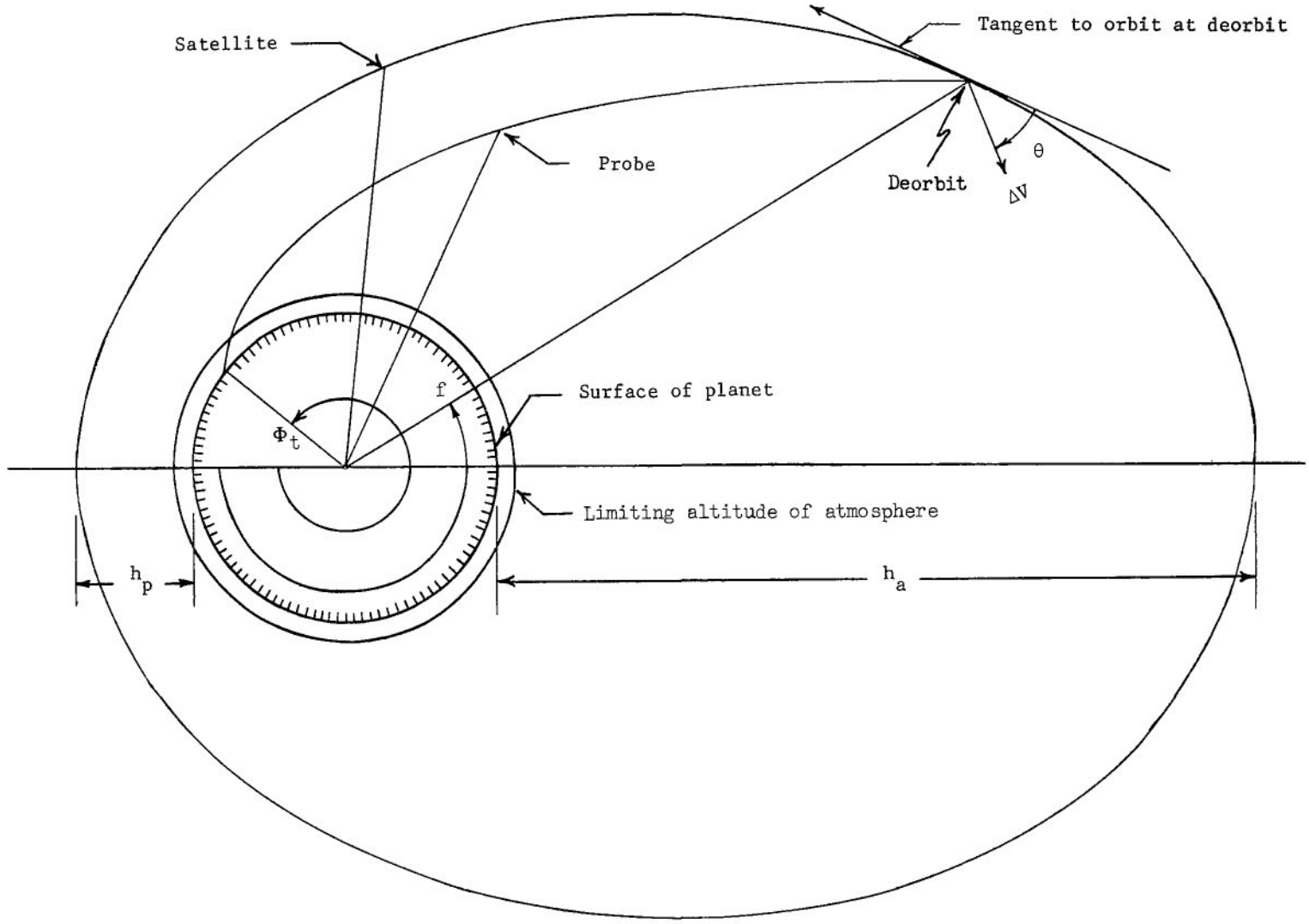

(a) Orbital geometry.

Figure 1.- Mission geometry.

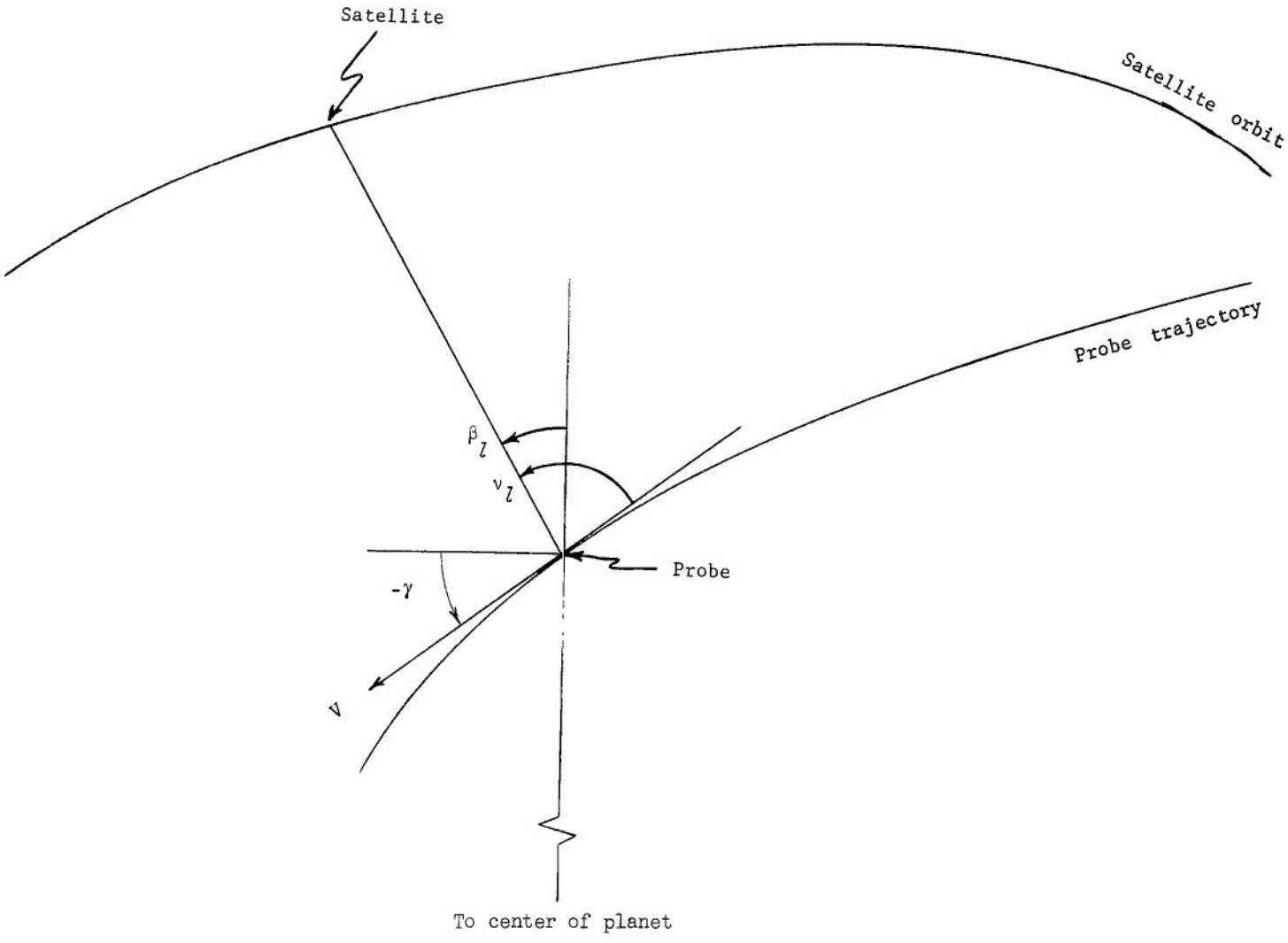

(b) Satellite-probe geometry.

Figure 1.- Continued.

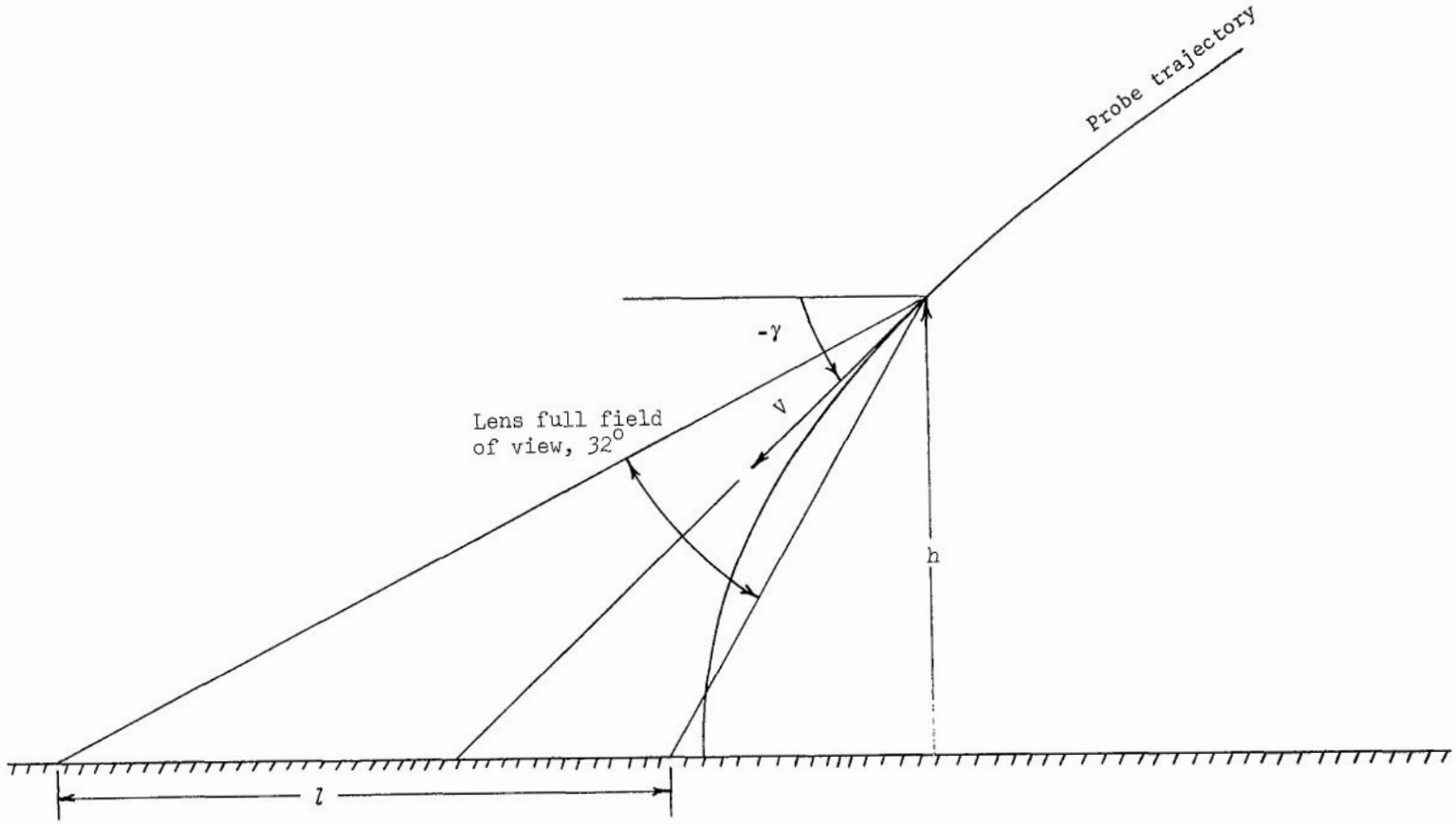

(c) Television geometry.

Figure 1.- Concluded.

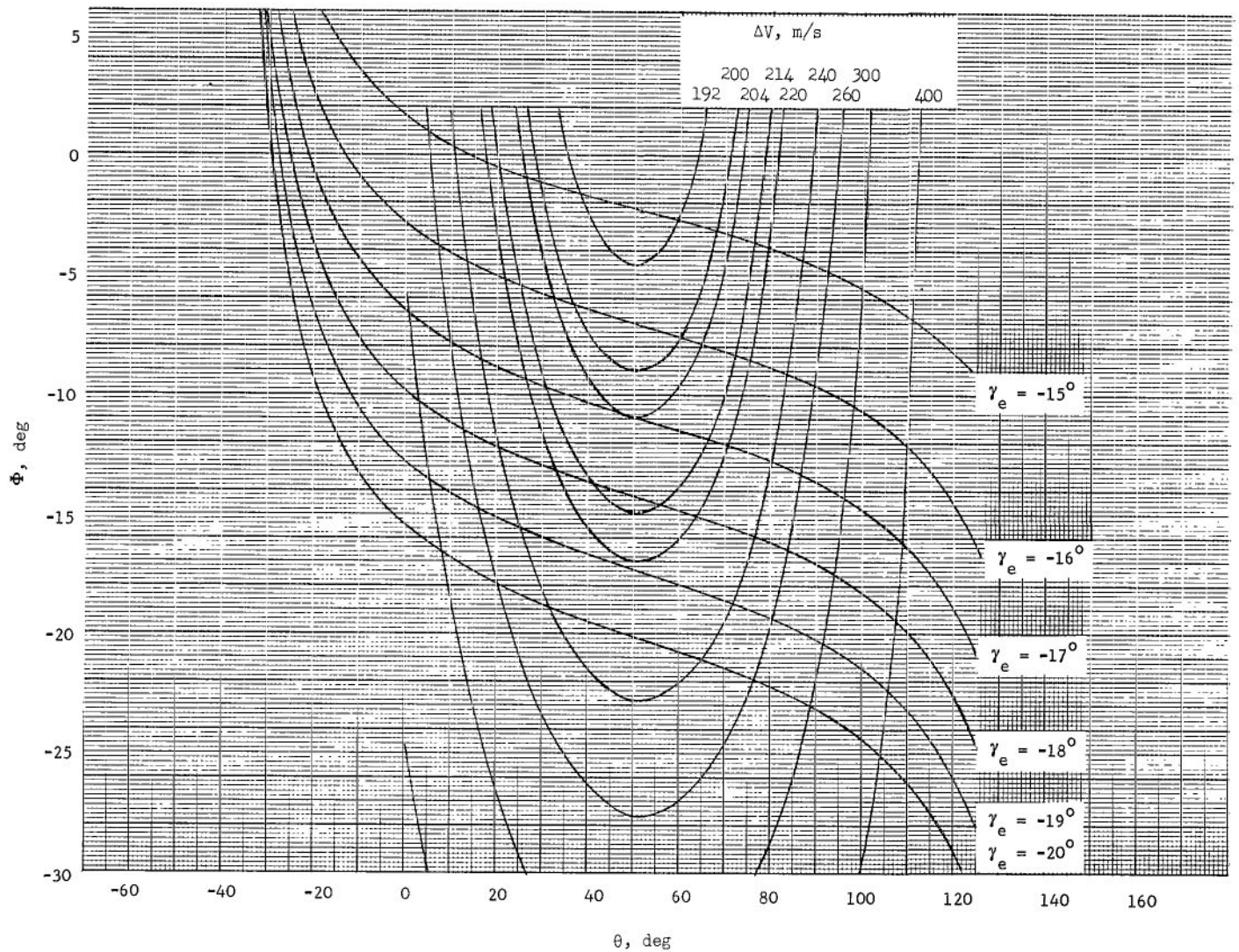

Figure 2.- Variation of vacuum landing point with deorbit velocity application angle for constant entry flight-path angles and constant deorbit velocities. h_p = 1000 km; h_a = 20 000 km; f = 240°.

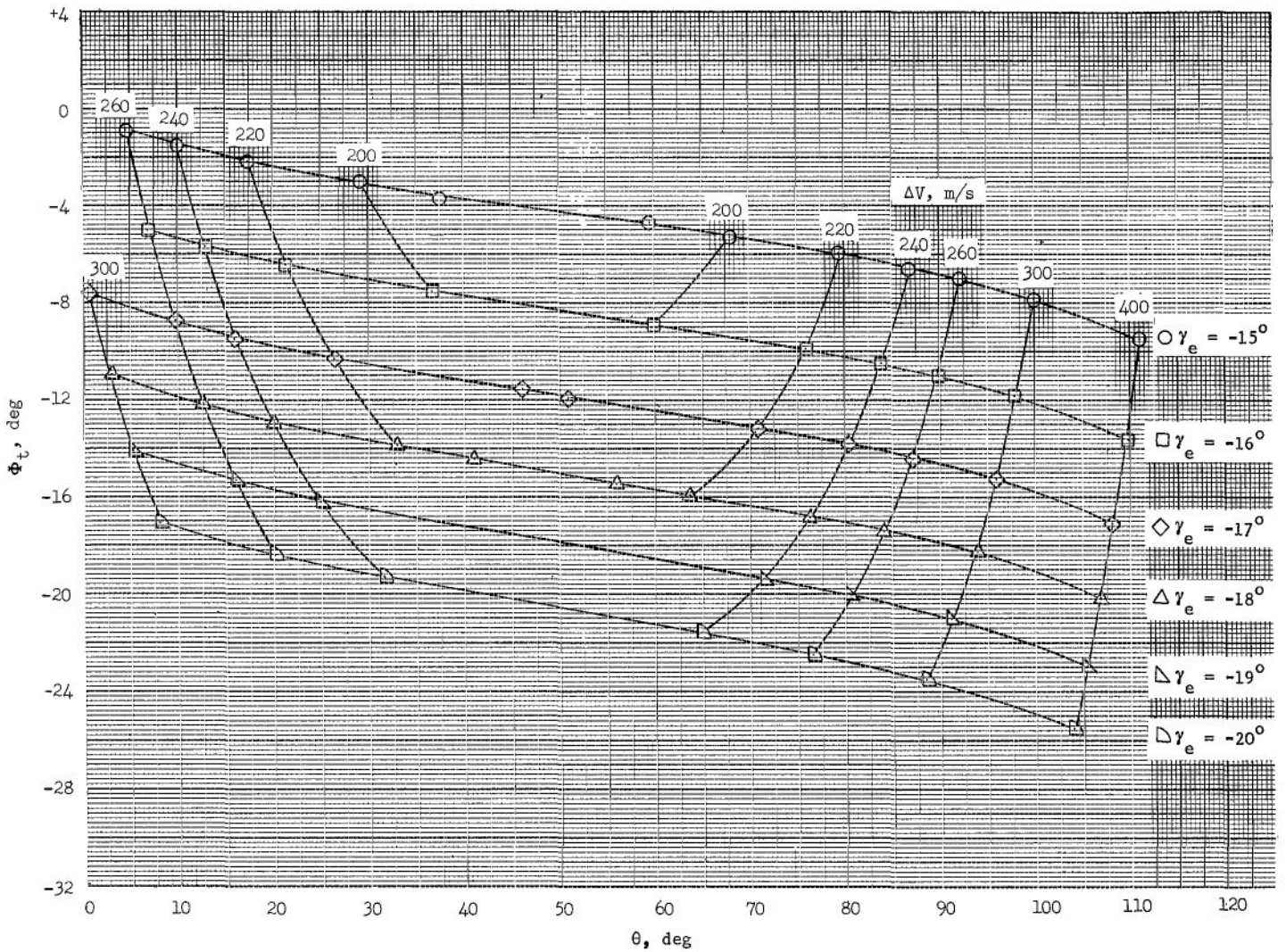

(a) Variation of true landing point with deorbit ΔV angle.

Figure 3.- Mars deorbit trajectory envelope for a probe descent through the VM-8 atmosphere. h_p = 1000 km; h_a = 20 000 km; f = 240°; m/C_DA = 39 kg/m^2 (0.25 slug/ft^2); $(m/C_DA)_d$ = 3.77 kg/m^2 (0.024 slug/ft^2); parachute deployment Mach number, 1.6; parachute release altitude, 1524 meters (5000 ft).

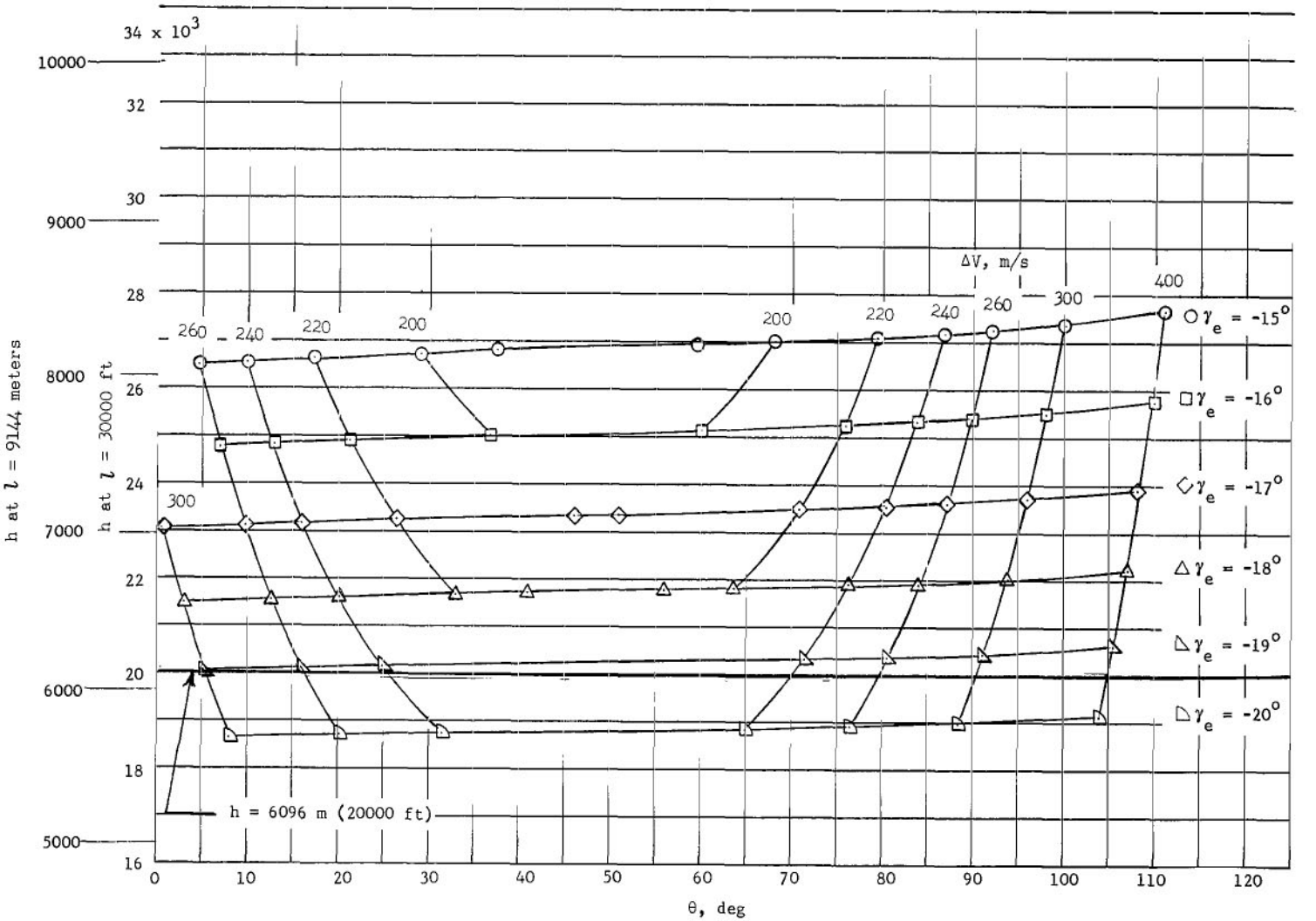

(b) Variation of altitude of probe at l = 9144 meters (30 000 ft) with deorbit ΔV angle.

Figure 3.- Continued.

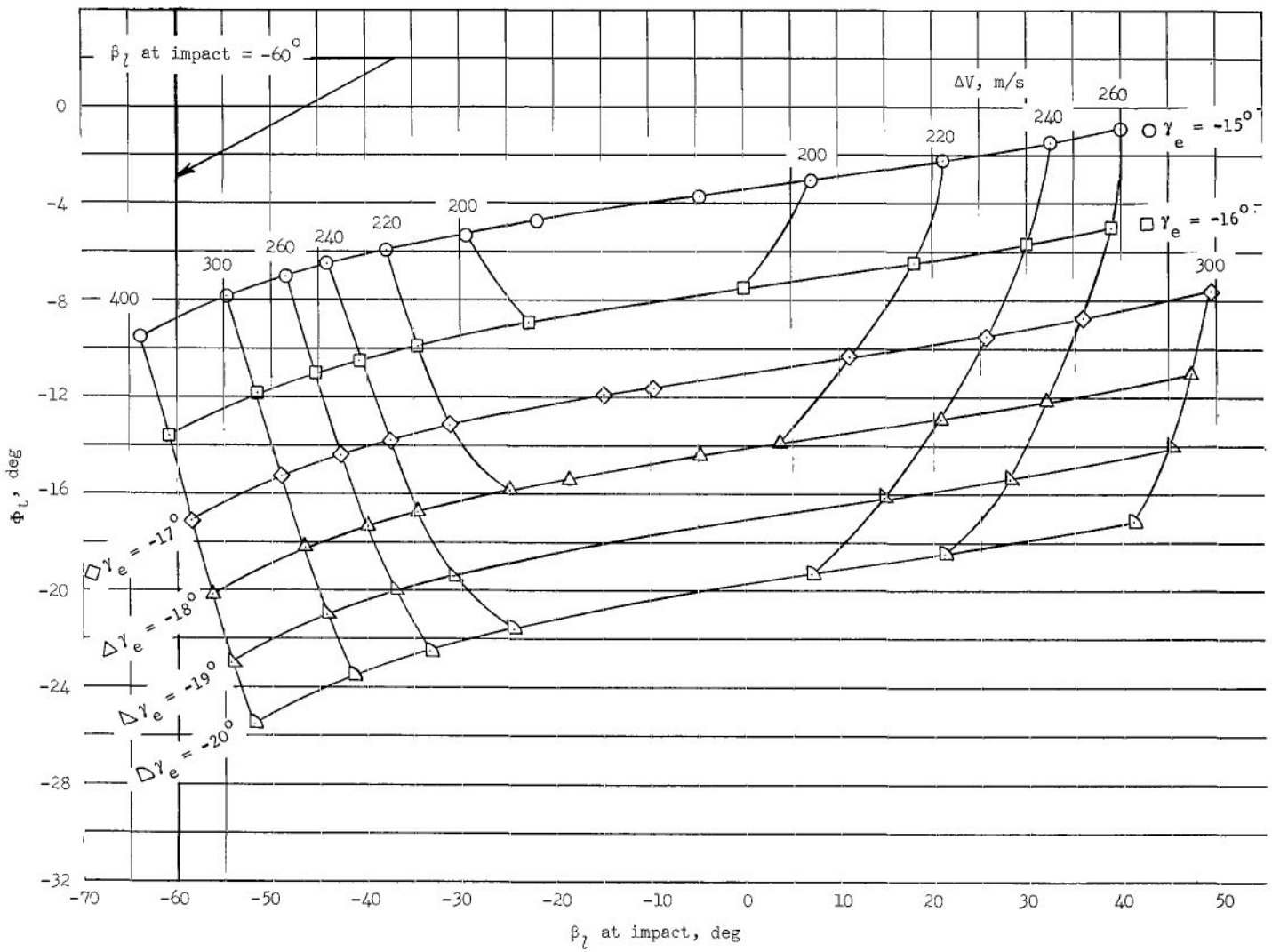

(c) Variation of Φ_l with β_l at impact.

Figure 3.- Continued.

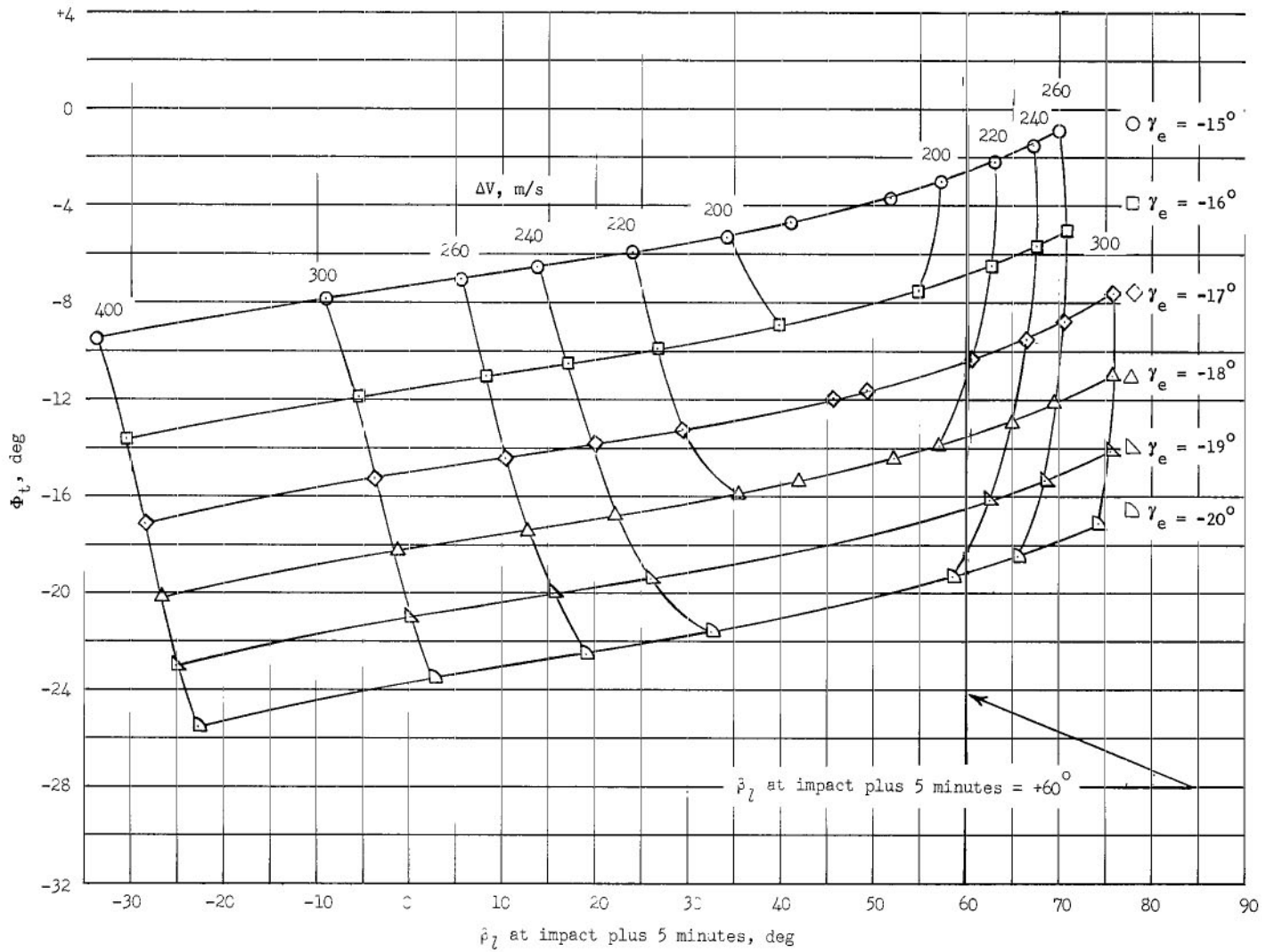

(d) Variation of Φ_t with β_l at impact plus 5 minutes.

Figure 3.- Continued.

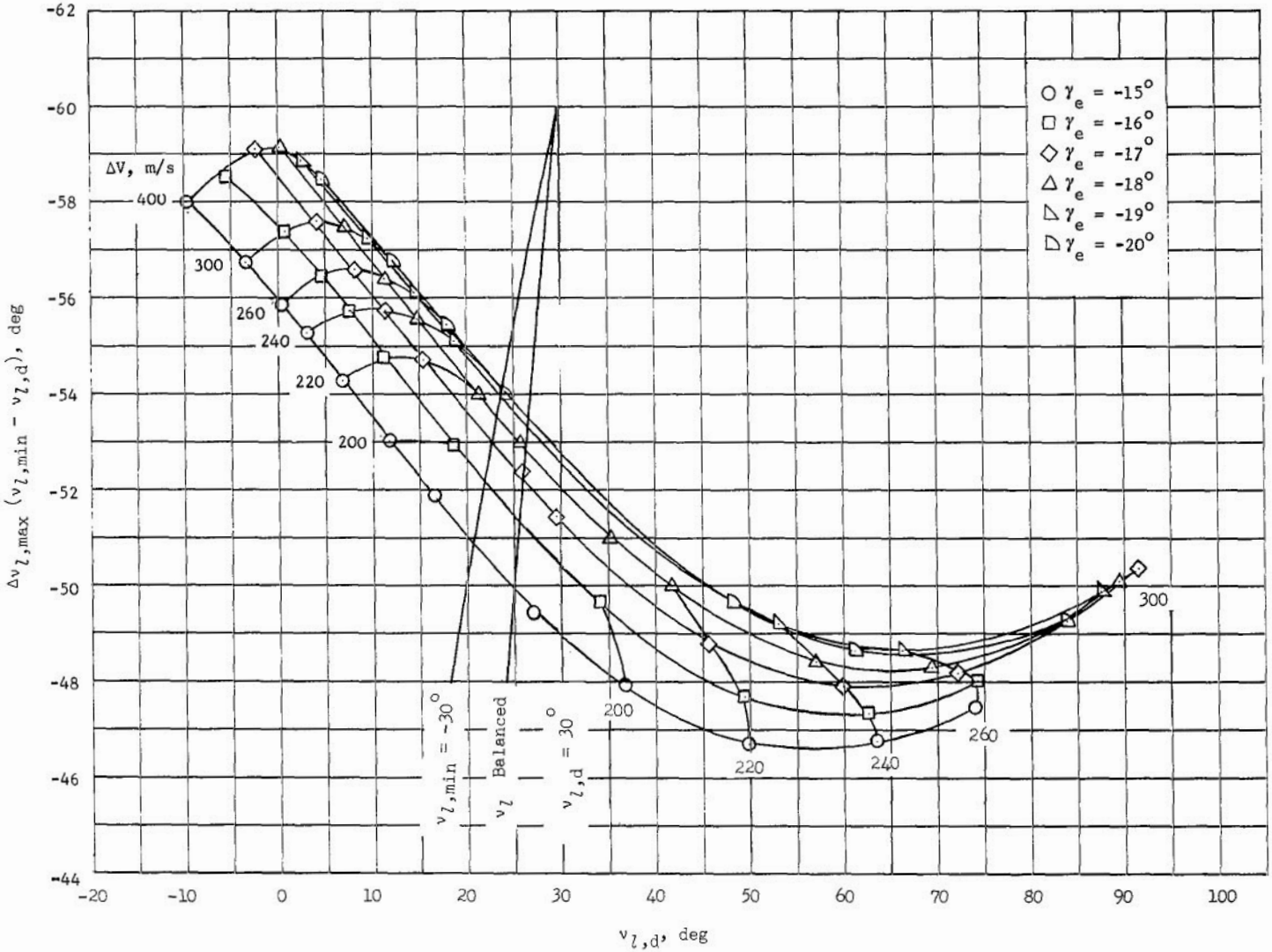

(e) Variation of $\Delta\nu_{l,max}$ with $\nu_{l,d}$.

Figure 3.- Continued.

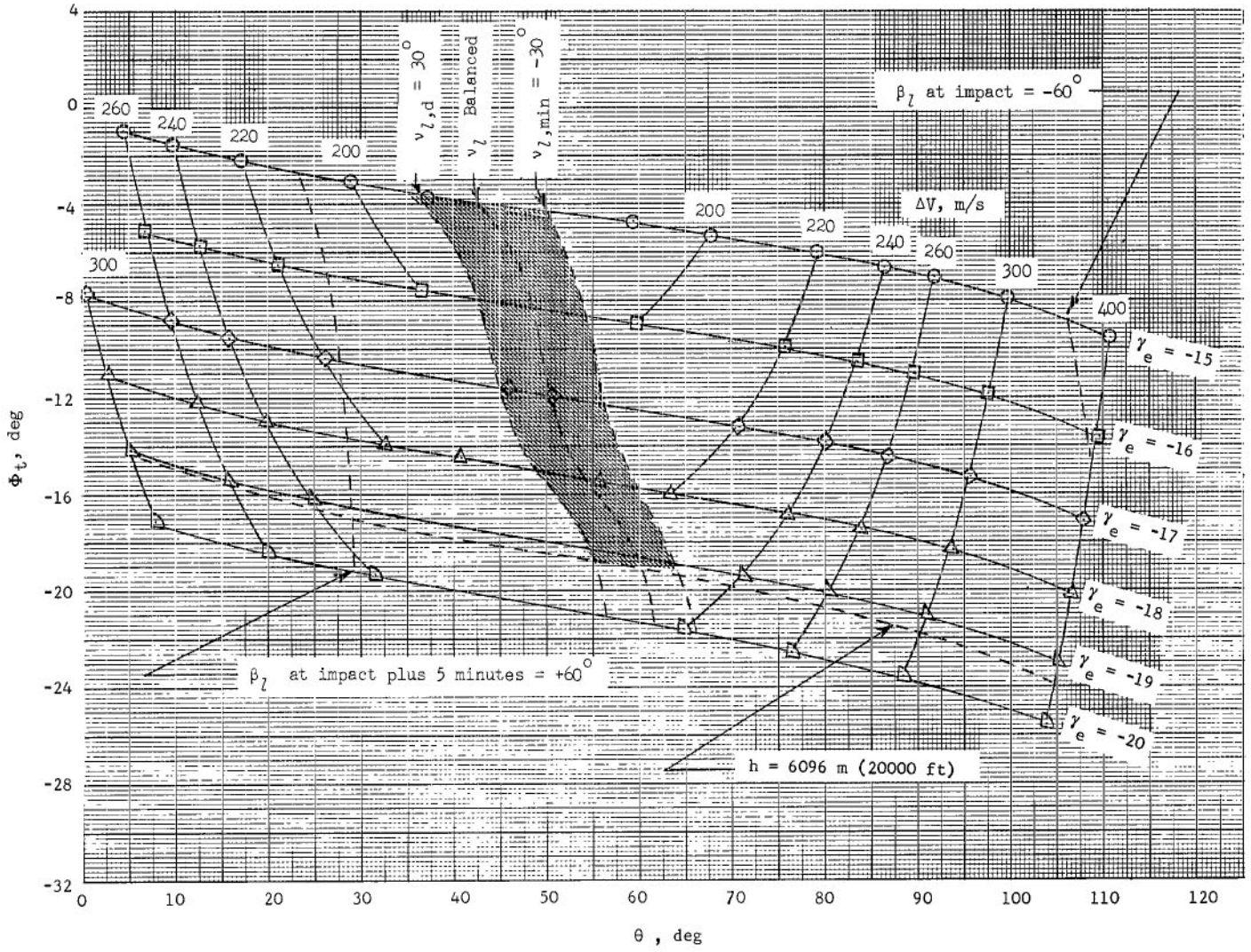

(f) Variation of Φ_t with θ with mission constraint lines.

Figure 3.- Concluded.

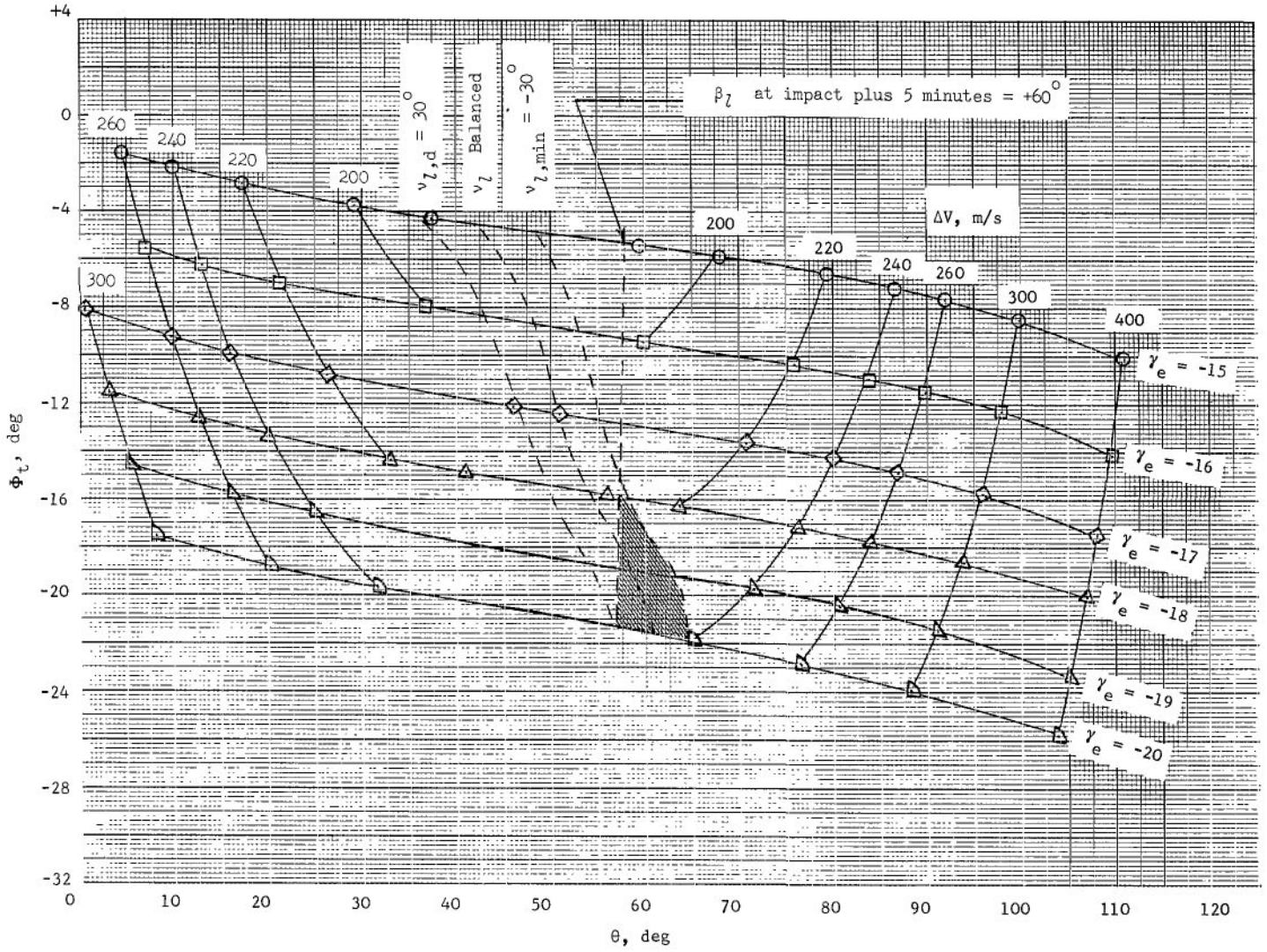

Φ_t vs θ with mission constraint lines

Figure 4.- Mars deorbit trajectory envelope for a probe descent through the VM-4 atmosphere. h_p = 1000 km; h_a = 20 000 km; f = 240°; m/C_DA = 39 kg/m^2 (0.25 slug/ft^2); $(m/C_DA)_d$ = 3.77 kg/m^2 (0.024 slug/ft^2); parachute deployment Mach number, 1.6, parachute release altitude, 1524 meters (5000 ft).

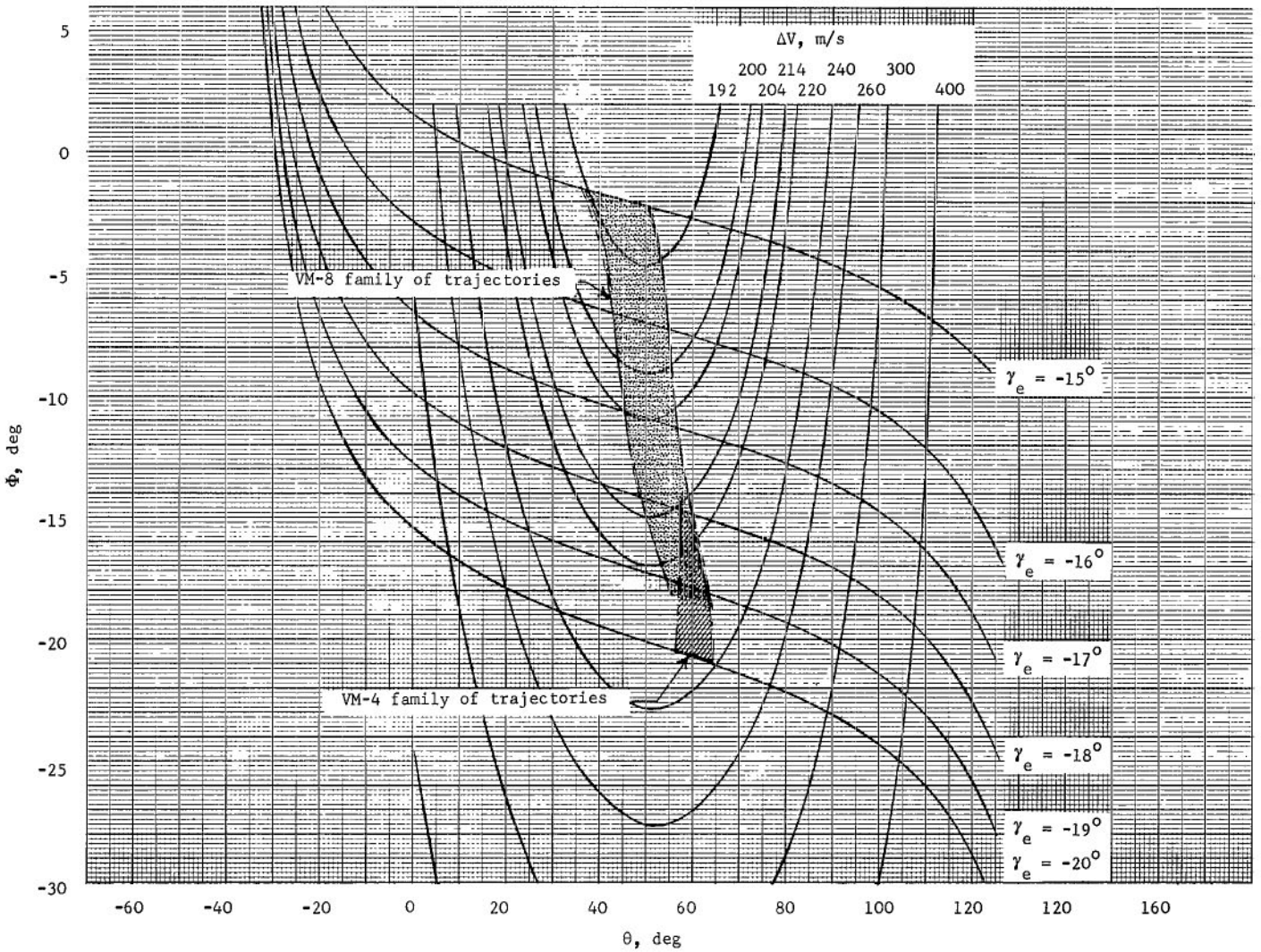

Figure 5.- Mars deorbit trajectories which satisfy the mission constraints for the range of atmospheres from VM-8 to VM-4. h_p = 1000 km; h_a = 20 000 km; f = 240°.

"The aeronautical and space activities of the United States shall be conducted so as to contribute . . . to the expansion of human knowledge of phenomena in the atmosphere and space. The Administration shall provide for the widest practicable and appropriate dissemination of information concerning its activities and the results thereof."

—NATIONAL AERONAUTICS AND SPACE ACT OF 1958

NASA SCIENTIFIC AND TECHNICAL PUBLICATIONS

TECHNICAL REPORTS: Scientific and technical information considered important, complete, and a lasting contribution to existing knowledge.

TECHNICAL NOTES: Information less broad in scope but nevertheless of importance as a contribution to existing knowledge.

TECHNICAL MEMORANDUMS: Information receiving limited distribution because of preliminary data, security classification, or other reasons.

CONTRACTOR REPORTS: Scientific and technical information generated under a NASA contract or grant and considered an important contribution to existing knowledge.

TECHNICAL TRANSLATIONS: Information published in a foreign language considered to merit NASA distribution in English.

SPECIAL PUBLICATIONS: Information derived from or of value to NASA activities. Publications include conference proceedings, monographs, data compilations, handbooks, sourcebooks, and special bibliographies.

TECHNOLOGY UTILIZATION PUBLICATIONS: Information on technology used by NASA that may be of particular interest in commercial and other non-aerospace applications. Publications include Tech Briefs, Technology Utilization Reports and Notes, and Technology Surveys.

Details on the availability of these publications may be obtained from:

SCIENTIFIC AND TECHNICAL INFORMATION DIVISION

NATIONAL AERONAUTICS AND SPACE ADMINISTRATION

Washington, D.C. 20546